Building and Environment 235 (2023) 110255

Contents lists available at ScienceDirect

Building and Environment

journal homepage: www.elsevier.com/locate/buildenv

Seasonal effects of thermal comfort control considering real-time clothing insulation with vision-based model

Eun Ji Choi, Young Jae Choi, Nam Hyeon Kim, Jin Woo Moon *

School of Architecture and Building Science, Chung-Ang University, 84, Heukseok-ro, Dongjak-gu, Seoul, 06974, Republic of Korea

ARTICLE INFO

Keywords:
Thermal comfort
Predicted mean vote
Clothing insulation
Occupant-centric control
Vision-based model

ABSTRACT

Occupant information is being actively introduced into building control to create a comfortable indoor environment and ensure effective building operation. The occupants' clothing information is a key factor influencing the thermal sensation and must be considered in comfort-based control. Considering these aspects, this study was aimed at comprehensively analyzing the influence of PMV-based control with real-time clothing insulation (R-CLO) on the thermal comfort and system power consumption in different seasons and attires. To this end, a vision-based R-CLO model was advanced, by including stages for person-detection and for garment detection and classification. PMV-based control with the R-CLO model was performed on seven ensembles of winter clothing. The winter experiment results were evaluated and compared with the summer results reported in the previous study to analyze the experimental findings by season. The error of the R-CLO model in estimating the clothing insulation was as low as 0.04 clo. Through PMV-based control considering real-time clothing insulation, the occupants' thermal comfort was enhanced in both summer and winter compared to the existing control methods. Additionally, each 0.1 clo reduction in summer saved average power consumption by 16%, whereas each 0.1 clo increase in winter reduced average power consumption by 13.7%. The existing control strategies appear to prioritize energy over comfort, particularly during the winter. Overall, real-time clothing information can be used for building system control to improve thermal comfort. Furthermore, this study indicates that additional research should be focused on enhancing the system's energy efficiency while appropriately considering the thermal comfort.

1. Introduction

The occupant information must be considered when assessing the indoor environment quality and building energy efficiency [1–3]. Building control based on accurate occupant information can promote the efficient use of building energy according to occupant needs [4,5]. With recent advancements in the internet of things and sensing technologies, researchers have focused on occupant-centric control (OCC), a building control strategy that takes into account the occupant information such as the presence, count, and preferences of occupants [4, 6–9]. OCC can help prevent inappropriate system operation while providing occupants with a customized comfort environment.

The thermal comfort and preferences of occupants must be considered in building control to minimize the occupant discomfort [10]. Among the models that quantitatively evaluate the thermal comfort, the predicted mean vote (PMV) is a representative index that is used worldwide [11–13]. In addition to environmental factors such as the air temperature (T_a), relative humidity (RH), mean radiant temperature (T_r), and air velocity (V_a), PMV takes into account the metabolic rate (M) and clothing insulation (I_{cl}) [14]. Comfort-driven control considering the PMV as a control variable is widely implemented in real buildings; however, the personal factors are typically set to an arbitrary default value [15–18]. If information regarding the occupants' activities and clothing is not considered, the use of PMV cannot ensure the comprehensive consideration of the thermal comfort. Therefore, it is necessary to measure dynamic personal factors to provide accurate information regarding the thermal comfort of occupants, and this aspect has been widely investigated [19–23].

Clothing insulation refers to the insulation value of the combination of individual garments worn by a person. This insulation is a dynamic variable that changes depending on the type, material, and layers of clothing and considerably influences thermal comfort and health [12, 24]. The exact insulation value of clothing can be measured using a thermal manikin in a thermal environment. However, this method is not suitable for the real-time measurement of every clothing item worn by

* Corresponding author.
E-mail addresses: ejjchl77@cau.ac.kr (E.J. Choi), chldudwo13@cau.ac.kr (Y.J. Choi), skagus1546@cau.ac.kr (N.H. Kim), gilerbert73@cau.ac.kr (J.W. Moon).

https://doi.org/10.1016/j.buildenv.2023.110255
Received 23 November 2022; Received in revised form 24 January 2023; Accepted 26 March 2023
Available online 28 March 2023

Nomenclature

T_a	air temperature [°C]
T_{set}	setpoint temperature [°C]
RH	relative humidity [%]
T_r	mean radiant temperature [°C]
V_a	air velocity [m/s]
I_{cl}	clothing insulation [clo or m^2 ˙K/W]
I_{clu}	garment insulation [clo or m^2 ˙K/W]
M	metabolic rate [met or W/m^2]
PMV	predicted mean vote
TSV	thermal sensation vote
TSVr	relative TSV
ASHRAE	American Society of Heating, Refrigerating and Air-Conditioning Engineers
ISO	International Organization for Standardization
OCC	occupant-centric control
DBT	dry-bulb temperature
R-CLO	real-time clothing insulation
CNN	convolutional neural network
YOLO	You Only Look Once
CNN	convolutional neural networks
B-box	bounding box
PTHP	packaged terminal heat pumps

occupants in real buildings [25,26]. Therefore, various approaches have been proposed for estimating the dynamic I_{cl} of an occupant in a building, such as data-driven models (i.e., regression model) [27–30] based on environmental factors or deep learning models based on thermal images [30–32] and RGB images [23,31,33–35] recorded using a non-invasive vision sensor. The RGB-image-based technique is a promising strategy for actual buildings because it can measure the I_{cl} indirectly and objectively in real-time without requiring occupant intervention.

Notably, to evaluate the practical applicability of the vision based I_{cl} estimation method, it is necessary to assess the influence of the comfort control based on the I_{cl} on the thermal comfort and system energy use. However, the existing research on PMV-based control in indoor environments using the vision-based I_{cl} estimation method is limited and being conducted recently [23,35]. Prior to conducting this study, the same research team of Choi et al. [22] assessed the effect of real-time clothing insulation on energy use and thermal comfort by the summer experiment. The authors demonstrated that the use of the real-time I_{cl} information can help enhance the occupants' thermal comfort, however, they did not perform a seasonal analysis. The effect of such control on the thermal comfort and power consumption may differ across seasons (owing to changes in the indoor clothing types and system operating conditions). Therefore, comparative analyses must be performed across seasons, including diverse garments to determine how the PMV-based control reflecting the actual I_{cl} affects the thermal comfort and power consumption.

The present study was aimed at experimentally analyzing the impact of real-time I_{cl} on the indoor thermal comfort and system power consumption during cooling and heating periods. The novelty of this study is that the additional experiment was conducted in the heating period and the experimental results were compared to those of the cooling season. By conducting comprehensive evaluations under various seasons and clothing conditions, the necessity of considering the real-time information of occupant clothing insulation is highlighted, and results that are generalizable across seasons are obtained.

For increasing its applicability to real buildings, the vision-based model for estimating real-time clothing insulation (R-CLO) developed by Choi et al. [23,36] was extended in this study by adding a function to detect individual occupants and enhancing the model performance. The classification performance of the model for winter clothing was enhanced, and comfort-based control was implemented with seven combinations of clothing. The results of thermal comfort and system energy use were compared with those obtained using existing control methods to verify the applicability and effectiveness of the proposed method in practical settings.

The process flow of this research can be summarized as follows (Fig. 1): The novelty of the proposed technique against the existing methods for estimating clothing insulation is highlighted (Section 2). The performance of the advanced R-CLO model re-trained on the augmented clothing dataset and control algorithm are evaluated (Step A), as discussed in Sections 3.1–3.2. Section 3.3 presents the experimental method (Step B). Section 4 presents the results of the experiment in winter settings, and the seasonal aspects are discussed in Section 5 by comparing the results of experiments in winter and summer settings.

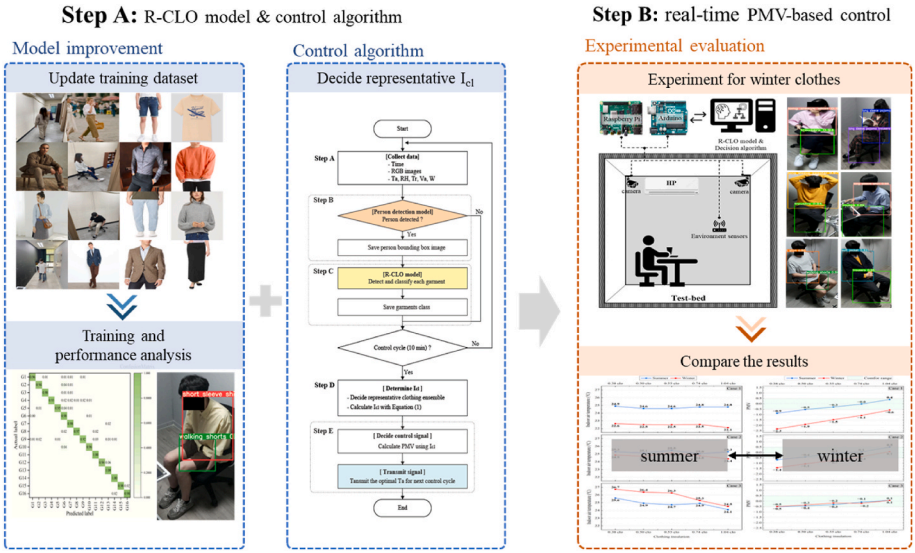

Fig. 1. Research process.

2. Literature review

This section describes the existing methods for estimating the clothing insulation. In addition, research on implementing comfort control based on the PMV (that reflects R-CLO) is described to highlight the novelty and significance of this study.

2.1. Methods to estimate the clothing insulation

The clothing considerably influence occupants' thermal comfort [12,24]. Therefore, precise information regarding the clothing insulation must be obtained to implement comfort-based building control. International standards such as ISO 9920 [37] and ASHRAE standard 55 [12] provide the thermal insulation values for different types of garments (such as daily and work attire) with different materials (I_{clu}), measured using thermal manikins.

Notably, in actual buildings, people may alter their clothing in response to psychological and social circumstances or a behavioral regulation based on the thermal sense [38]. Real-time measurement of I_{cl} is challenging because it requires expensive equipment, time, and intervention of the occupants. Therefore, various studies have focused on measuring or estimating the clothing insulation.

In the early research on I_{cl} estimation, data-driven regression models were developed to predict the mean daily I_{cl} based on environmental data such as external temperature (on average or specific time), operating temperature, and dew point temperature [27,28,30,39]. These models could obtain the representative I_{cl} of one day, which was an improvement over the traditional approach in which an arbitrarily chosen constant value was applied. Nevertheless, the model accuracy was limited, and these models could not be used for time-based control. Therefore, to replace the daily average value, a new method for estimating the I_{cl} across time periods is necessary.

Recently, various modeling techniques such as deep learning and computer vision have been applied to measure the I_{cl} in real-time. In these techniques, an image, typically, a thermal or an RGB image, is used as the input variable. Lee et al. [31] and Liu et al. [21,34] used thermal images to estimate the I_{cl} based on the skin and clothing temperatures. In addition to the thermal images, numerous studies have been conducted to categorize different types of clothes using RGB images [23,35,40–42]. In most of these studies, the type, weight, or covered body surface area of clothes in an image were assessed using a computer vision technique based on convolutional neural networks (CNNs). Dziedzic et al. [41] presented a method for determining the clothing factor by recognizing the area of clothing surface, and Watanabe et al. [42] proposed a new approach for calculating I_{cl} by estimating the weight of clothes from an image. Additionally, Choi et al. [35] presented a vision-based model that classified five clothing combinations with an average accuracy of 86%.

Notably, in the existing studies, a person's entire clothing ensemble was categorized into a single class [35], or the top category was the only class that included classifiable garments [21,34]. Recently, Choi et al. [23,36] developed an R-CLO model that can estimate the I_{cl} of various combinations of clothing based on RGB images, by individually classifying garments such as tops and bottoms. The model exhibited an average I_{cl} error for the entire ensemble for 0.03 clo. Based on this model, an extended R-CLO model is developed in this study, which is expected to be more practical as it includes a person detection stage to enhance the model performance.

2.2. Comfort control based on clothing insulation

The PMV index is the most widely used variable for comfort control. However, I_{cl} is typically set to 0.5 clo in summer and 1.0 clo in winter [16,43]. As described in Section 2.1, various methods to measure I_{cl} have been developed. However, research on comfort-based control considering real-time I_{cl} is limited [23,35].

In the existing studies on comfort-based control with the R-CLO framework, a vision-based model with high field applicability was used [23,35]. According to tests on PMV-based HVAC control using real-time I_{cl} for six male participants in three ensemble scenarios, the thermal comfort is higher than that achieved using conventional PMV control with default I_{cl} values [35]. However, to emphasize the effect and utility of clothing information for comfort control, it is necessary to derive results with a larger number of participants and various clothing combinations. To this end, a comfort-based control experiment with the R-CLO model was conducted in summer with 15 participants and nine clothing combinations by Choi et al. [23]. These experiments helped clarify the influence of the R-CLO on the system's power consumption and occupants' thermal comfort. The results demonstrated that the participant's PMV and thermal sensation vote (TSV) were improved when the R-CLO was considered, and the system consumed more power as I_{cl} increased.

Nevertheless, additional experiments must be performed for heating periods and a comparative analysis must be performed for seasonal data because the indoor clothing types and system operating conditions vary across seasons. Therefore, to determine the variations in the thermal comfort and power consumption across seasons, a comfort control experiment based on the R-CLO was conducted in this study.

3. Methods

This section describes the main process and conditions of the experiment. The updated R-CLO estimation approach, which consists of the occupant detection and garment classification stages, is described in Section 3.1.1. The advanced R-CLO model, which outperforms the original model in terms of winter clothing, is described in Section 3.1.2. Section 3.2 describes a system control algorithm based on PMV with R-CLO. The experimental methodology, including sensor equipment, control mechanism, process, and participant information, is described in Section 3.3. To ensure a fair comparison with the experiment conducted during the cooling period, the experimental procedures and basic conditions were the same as those adopted in the previous study [23].

3.1. Estimation of real-time clothing insulation

3.1.1. Process of R-CLO estimation

The R-CLO model can classify specific types of clothing worn by an individual in real-time from an RGB image captured by a camera. However, to apply this model to an indoor environment with multiple occupants, it is necessary to detect occupants before estimating the I_{cl} value for each person [21].

Accordingly, the R-CLO estimation process was divided into two stages, as shown in Fig. 2. Stage 1 was aimed at detecting individuals in the image and cropping the background to generate a human bounding box (B-box) image. In Stage 2, every piece of garment worn by a person in the B-box were detected, and the types of the individual garments were classified. Through the addition of Stage 1, these two objectives can be satisfied: 1) infer the exact clothing combination worn by a specific occupant; 2) estimate the I_{cl} for each person in multi-occupant situation. These functions demonstrate the high applicability of the model.

You only look once (YOLO) v5 [44] was used as the main network structure for both stages. By replicating the human visual system, the CNN-based YOLO network that processes two-dimensional data can detect objects with only one image. This network can be applied for the real-time estimation of the occupant I_{cl} in actual buildings as it can rapidly detect objects. Therefore, YOLOv5 network was used for model development in this study. The released YOLOv5 network [44] containing trained parameters was used in Stage 1. In Stage 2, only the YOLOv5 structure with no trained parameters was used, and it was trained with diverse clothing image data to allow it to detect and classify individual garments.

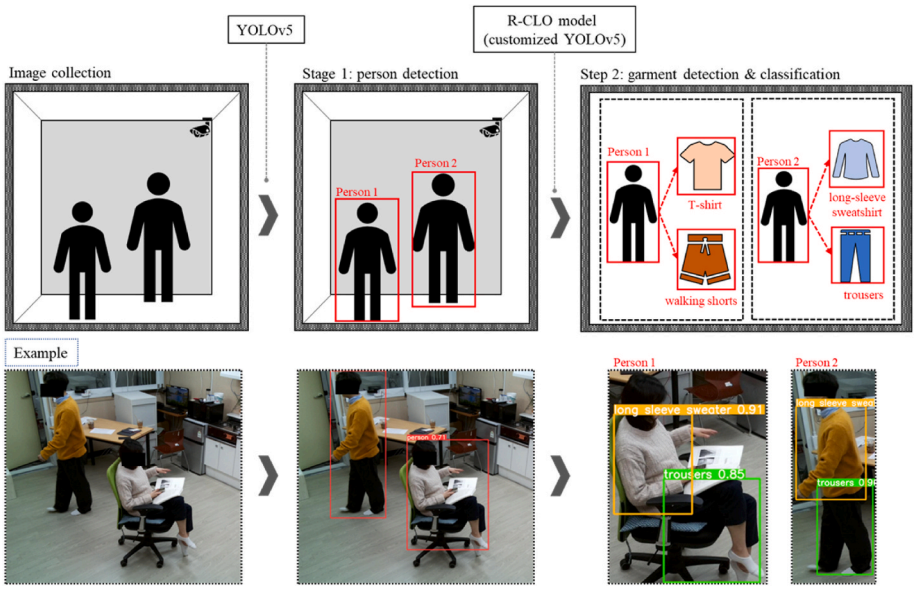

Fig. 2. Vision-based R-CLO estimation process.

3.1.2. Advanced R-CLO model for winter clothes

In this study, an advanced R-CLO model was developed by retraining the initial R-CLO model [23] on additional winter clothing data. To enhance the model performance for the heating period experiment, additional data for winter clothing were collected. The advanced model was retrained with the increased image dataset including garments with high insulation value such as a long-sleeve shirt, a long-sleeve sweatshirt, a long-sleeve sweater, trousers, an ankle-length skirt, sweatpants, and a long-sleeve shirt dress.

Table 1 is presented to indicate the performance improvement of the target classes through additional training. Before being trained over the additional dataset, the performance of the initial R-CLO model [23] for winter clothes was low, as indicated in Table 1. The performance of the advanced R-CLO model for most of the garment type was improved to that of the initial model. Notably, the 16 garments that the R-CLO model was expected to classify were selected based on the typical garments presented by ISO 9920 [37] and ASHRAE standard 55 [12]. The 16 garments, divided into five representative categories, include Top (G1: short-sleeve shirt, G2: long-sleeve shirt, G3: t-shirt, G4: long-sleeve sweater, G5: long-sleeve sweatshirt); Bottom (G6: trousers, G7: knee-length skirt, G8: ankle-length skirt, G9: walking shorts, G10: sweatpants); Outer (G11: suit jacket); Dress (G12: long-sleeve shirt dress, G13: short-sleeve shirt dress); and Pajamas (G14: long-sleeve pajama top, G15: pajama trousers, G16: short-sleeve pajama top).

Based on the test dataset, the advanced R-CLO model exhibited an average accuracy of 96.8% and over 92% for all clothing categories, as indicated in Table 1. Compared with that of the initial model [23], the average accuracy was more than 2.0% higher, and the classification performance for each garment was up to 13% higher (G12).

This R-CLO model can flexibly consider various cases of potential clothing combinations because it determines the total I_{cl} depending on the individual garments worn by the occupants. Thus, in this study, the model could classify maximum 34 combinations of clothes involving different classifiable garments (i.e., 6 of Top & Outer $\times$ 5 of Bottom + 2 of Dress + 2 of Pajama sets). This approach was more realistic than the existing method [31,34,35] that can classify only a particular outfit combination. Among the 16 garments that the model could classify, the representative clothing ensemble for the heating experiment was set up, as indicated in Table 2. These ensembles were selected based on the clothing type and insulation values presented in Tables A and B of ISO 7730 [11] to attain a clothing combination typically worn in offices. The highest I_{cl} was set as 1.34 clo because the experiment was conducted in winter, and thicker clothing than that used in the summer experiment was introduced.

The clothing used in the experiment is shown in Fig. 3. The 11 types of apparel that constitute the ensembles presented in Table 2 are short-

Table 1
Garment types and model training performance.

Label	Garment type	Accuracy of the R-CLO model	
		Initial model [23]	Advanced model (proposed)
G1	short-sleeve shirt	0.96	0.96
G2	long-sleeve shirt	0.93	0.94
G3	t-shirt	0.98	0.98
G4	long-sleeve sweater	0.88	0.93
G5	long-sleeve sweatshirt	0.90	0.94
G6	trousers	0.97	0.98
G7	knee-length skirt	0.97	0.98
G8	ankle-length skirt	0.94	0.97
G9	walking shorts	0.96	0.92
G10	sweatpants	0.92	0.96
G11	suit jacket	1.00	1.00
G12	long-sleeve shirt dress	0.81	0.94
G13	short-sleeve shirt dress	1.00	1.00
G14	long-sleeve pajama top	1.00	1.00
G15	pajama trousers	0.96	0.98
G16	short-sleeve pajama top	0.98	0.98

Table 2
Clothing ensembles for the winter season.

Ensemble	Clothing insulation (I_{cl})	Combination of garments
E1	0.38 clo	t-shirt (G3), walking shorts (G9)
E2	0.50 clo	short-sleeve shirt (G1), walking shorts (G9)
E3	0.55 clo	ankle-length skirt (G8), long-sleeve sweatshirt (G5)
E4	0.63 clo	long-sleeve pajama top (G14), pajama trousers (G15)
E5	0.74 clo	long-sleeve shirt (G2), trousers (G6)
E6	1.04 clo	long-sleeve shirt (G2), trousers (G6), long-sleeve sweater (G4)
E7	1.34 clo	long-sleeve shirt (G2), trousers (G6), long-sleeve sweater (G4), suit jacket (G11)

Essential clothes: underwear, ankle socks, sneakers.

Fig. 3. Garments used in the experiment.

sleeve shirt (G1), long-sleeve shirt (G2), t-shirt (G3), long-sleeve sweater (G4), long-sleeve sweatshirt (G5), trousers (G6), ankle-length skirts (G8), walking shorts (G9), suit jackets (G11), long-sleeve pajama top (G14), and pajama trousers (G15). Different clothing items were purchased based on the participants' gender and size, but the fabric composition was chosen to be as similar as possible to the insulation conditions specified in ISO 7730 [11]. Table A2 in Appendix A presents detailed information of the experimental clothing, including the type and fabric. In the experiment, the same essential apparel was worn with each outfit: ankle socks, footwear, and underwear.

Although the performance of the developed model was assessed over the test dataset, the performance can be differ with the application conditions, such as the image resolution, angle, and background. Therefore, a pre-test was performed to validate the performance of the advanced R-CLO model in the same test bed where the winter experiment was performed for the clothing conditions in Table 2. The assessment was performed using images recorded once every 5 s while each ensemble was worn for 10 min. The pre-test involved five participants who maintained a sitting posture on the test bed. The collected images were fresh data that were not included in the training and testing datasets, allowing the assessment of the model performance in a new environment.

Fig. 4 shows the experimental findings in comparison with those of the initial R-CLO model [23]. Based on further training on winter clothing, the advanced R-CLO model updated weights and biases, and the overall average accuracy was approximately 6% higher than that of the initial model. An accuracy of more than 80% was achieved for 8 of the 11 garments, and the accuracy for the long-sleeve sweater increased by more than 79%. Nevertheless, the performance of the proposed model for certain garments, such as pajama trousers, was lower (17%) than that of the initial model. This phenomenon occurred because the variation in the model parameters resulted in a higher percentage of incorrect classifications of "trousers" against "pajama trousers". However, the difference in insulation was only 0.05 clo, because the two garments have comparable shapes and insulation areas. Therefore, it was considered important to clarify how these results affect the I_{cl} value (which is used to calculate the PMV), as discussed in Section 4.1.

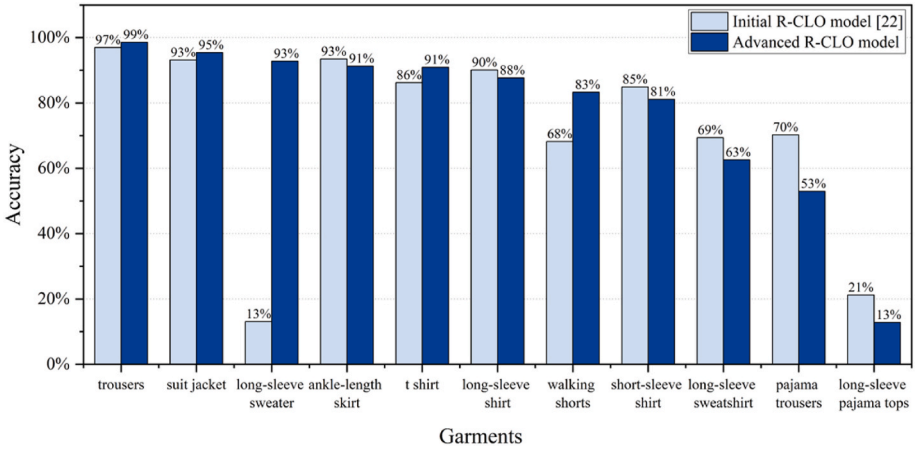

Fig. 4. Performance of R-CLO model for winter clothes applying to test bed.

3.2. R-CLO model-based control algorithm

The effects of potential errors will be reflected to the control as is if every I_{clu} data point from the R-CLO model is used for system control. Therefore, system control must be performed by selecting the I_{cl} value representing a certain control period and minimizing the impact of the classification error. To determine the I_{cl} representing the control cycle and to control the system based on the PMV with real-time clothing information, a control algorithm that includes the R-CLO model was developed (Fig. 5).

This control algorithm involves the following steps: In Step A, the time information, indoor RGB images, environmental data (T_a, RH, T_r, V_a) and system power usage (W) are collected in units of 15 s. In this study, the data collection time was set considering the socket communication stability of the camera sensor used in the experiment. Among the collected data, the RGB image is input to the person-detection model in Step B, and if an occupant exists, the B-box image of the detected person is saved. If an occupant is detected, Step C is implemented, i.e., the B-box image is used to classify each garment that the occupant is wearing using the R-CLO model. The advanced R-CLO model is embedded in Step C. If there is no occupant, Step C is skipped. Steps A through C are repeated throughout the control cycle (10 min), and the results are saved to the server in real-time.

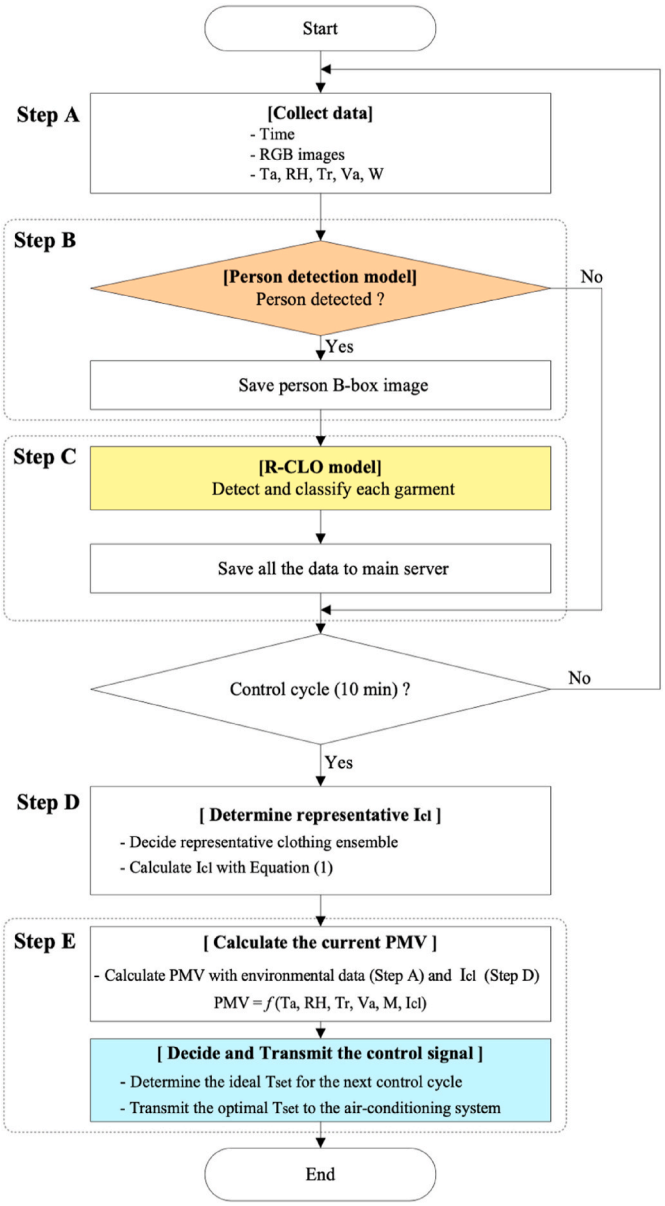

Fig. 5. R-CLO model-based control algorithm.

A representative I_{cl} is chosen at the end of each cycle by combining the ensemble with the most frequently classified garments for 10 min (Step D). For instance, if the classification percentages of t-shirt (Top) and working shorts (Bottom) are 95% and 93%, respectively, the occupant's entire outfit is regarded as an ensemble of t-shirt and working shorts, and the representative I_{cl} of that cycle is 0.38 clo. The total I_{cl} is obtained using Equation (1) recommended by ISO 9920 [37], with reference to the work of McCullough et al. [45]. In numerous field studies in which direct measurement was rendered challenging, the clothing insulation has been estimated using Equation (1) [46,47].

$$I_{cl} = 0.161 + 0.835 \sum I_{clu} \quad (1)$$

In Step E, the PMV of the current control cycle is calculated using the representative I_{cl} obtained in Step D and average values of the indoor environmental variables collected in Step A. Based on the calculated PMV, the ideal setpoint temperature (T_{set}) that will produce PMV = 0 for the next control cycle is determined. Assuming that the current environmental and individual variables are maintained except for T_a and T_r (T_r is set to have the same value as T_a) the temperature that is closest to PMV = 0 is chosen as T_{set} within the operating range of the heat-pump (18–30 °C). Lastly, an IR signal containing the newly constructed T_{set} is transmitted to the air-conditioning system. For example, if the environmental data in Step A are T_a: 20 °C, RH: 40%, T_r: 21 °C, V_a: 0.01 m/s and the personal data are M: 1.0 met, I_{cl}: 0.74 clo (from Step D), the current PMV is −1.4. Assuming T_a and T_r are equal, a value between 18 °C and 30 °C is input to identify that with the PMV closest to 0. This value is set as T_{set} for the next control cycle. In the considered example, the next T_{set} is 25 °C.

3.3. Experiment

3.3.1. Process

Fig. 6 schematically represents the test bed configuration and details of the sensors, air-conditioning system, and system control methods. The experiment was conducted in the same test bed as that used in the summer experiment. Two rooms measuring 2.7 m × 2.0 m × 2.2 m constituted the test bed inside the building. A server was placed outside of the room to collect data and control the system with the R-CLO model-based control algorithm.

Each room had an integrated sensor module for collecting information regarding the indoor environment, RGB images, and current data of the air-conditioning system. Fig. 6 shows each sensor and its specifications. The camera sensor installed at a height of 1.7 m simultaneously gathered images from two angles, and the environment sensors placed in the middle of the indoor wall at a height of 1.2 m measured the indoor T_a, RH, T_r, and V_a. The power meter connected to the air conditioning system measured the electric current data. All sensors were calibrated before the experiment. Raspberry Pi and Arduino, single-board computers capable of TCP/IP communication and real-time data collection, were used to store the data every 15 s in the server. The server determined a control signal for each control cycle based on the stored data and transmitted it to the IR sensor installed next to the system.

Inverter-type packaged terminal heat pumps (PTHP) were installed in the test bed for heating and cooling, in the room's upper left corner. PTHP, a wall-mounted product, has a coefficient of performance of 3.64 (cooling) or 3.89 (heating), capacity of 2.80 (cooling) or 3.50 kW (heating), and power consumption of 0.77 (cooling) or 0.90 kW (heating), respectively. The system had an on/off control scheme that could regulate the indoor temperature with a 2 °C deadband of the setpoint.

Three control methods were established, as shown in Fig. 6. Cases 1 and 2 were traditional system control methods that have been

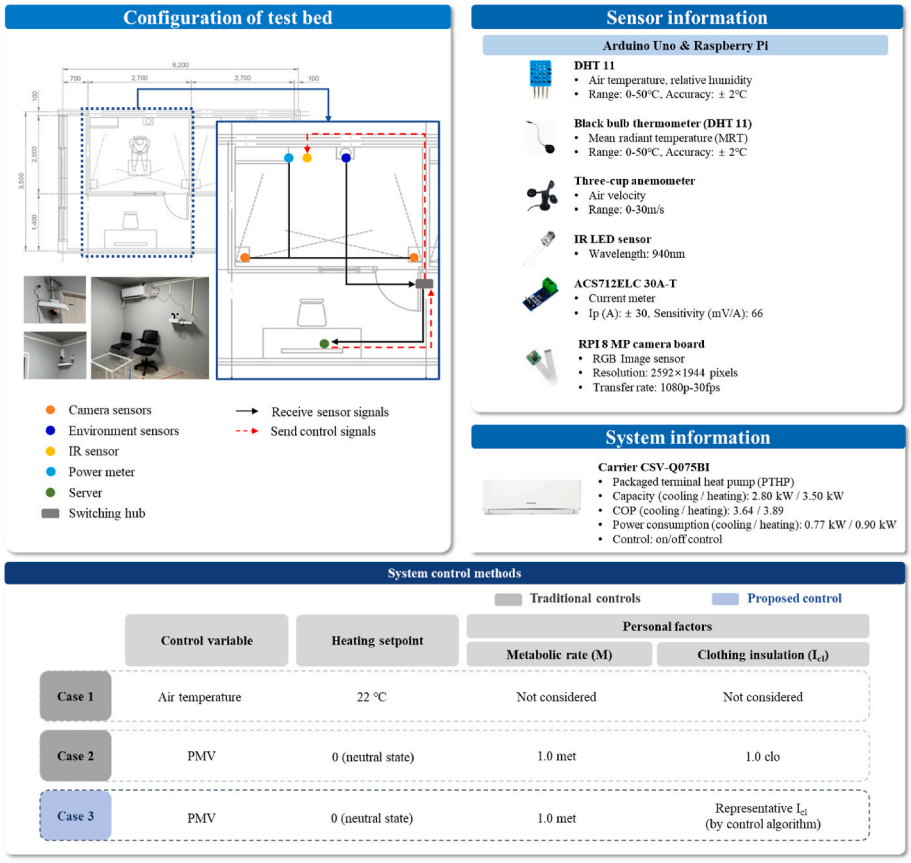

Fig. 6. Experiment setup.

commonly applied in buildings, and Case 3 was the proposed control method based on the R-CLO. Specifically, Case 1 controlled the system based on the dry-bulb temperature (DBT). Only the room temperature was measured and regulated in accordance with the heating setpoint of 22 °C. Case 2 involved comfort control based on the PMV. The PMV was calculated using the measured environmental variables T_a, RH, T_r, and V_a, but the two personal factors were set as 1.0 met and 1.0 clo. Case 3 used a PMV-based comfort control strategy as well. However, the clothing insulation was estimated in real-time with the R-CLO model, whereas M was set as 1.0 met. The setpoint in Cases 2 and 3 was set as PMV 0.0.

The experiment was conducted for 40 min for each ensemble listed in Table 2, and the control cycle was set as 10 min. At 10, 20, and 30 min, the room temperature was adjusted by receiving a control signal in accordance with the control methods. The participants sat in the middle of the test bed during the experiment for maintaining M at 1.0 met and performed tasks such as reading, writing, and observing. The participants were dressed as required according to the ensemble condition.

3.3.2. *Participant information*

Twenty-three participants were recruited, including 12 males and 11 females aged 20–30 y. Table 3 presents the information of the participants. People with a BMI in the normal range (18–23 kg/m^2) were enlisted to eliminate the influence of the BMI on the thermal comfort. In the clothing ensemble, one additional case E3 was included for female participants. Therefore, the experiments for the female and male participants were conducted for 840 and 720 min, respectively. The experiment was performed in winter 2022, from January to March. The subjective TSV of the participants were measured and compared with the estimated PMV. A point-in-time survey (among the thermal sensation surveys of ASHRAE standard 55) was administered to determine the TSV [12], and Google Forms were used to collect the participants' TSVs at 2-min intervals.

Before the experiment, the participants performed an additional test for 5 min to examine their relative TSV (TSVr). The participants wore a clothing ensemble corresponding to 1.0 clo (brief/bras and panties, socks, sneakers, long-sleeve shirt, trousers), and their TSV was measured once every minute for 5 min at a temperature of 22 °C, which is a typical T_{set} of DBT-based control in winters. According to the most frequently occurring data for 5-min, both male and female participants report feeling comfortable (TSVr = 0), with the exception of one male participant who reported feeling "slightly cold" (TSVr = −1). Overall, most participants felt similarly warm and were thermally neutral at the same conditions of 22 °C and 1.0 clo. Detailed information of the recruited participants and pre-test results is presented in Table A1.

Table 3
Participant information.

	Height (cm)		Weight (kg)		BMI (kg/m^2)		Age	
	Mean	SD[a]	Mean	SD	Mean	SD	Mean	SD
Male	173.9	5.4	65.7	7.1	21.7	2.0	25.0	2.9
Female	160.6	4.8	51.3	5.2	19.8	1.4	23.9	2.6

[a] SD: Standard Deviation.

4. Results of the winter experiment

This section describes the results of experiments performed in the heating period. Section 4.1 discusses the accuracy of the R-CLO estimation for Case 3, and Section 4.2 describes the thermal environment and power consumption for seven clothing ensembles.

4.1. Performance of the R-CLO estimation

The performance of the human detection model was assessed in multiple occupancy situations before applying it in the experiment. The evaluation was conducted in a sperate mockup setting that was not used for training, and the number of occupants was increased from one to three. The average person detection accuracy of the model was 95%. In other word, the model could accurately detect humans in cases involving 2–3 occupants. The model accuracy was more than 99% in the Case 3 experiment conducted on a single occupant. This high performance could be attributed to the clean background and absence of any elements in test bed that may complicate the detection of occupants. Overall, in most instances, an occupant was detected, and the cropped B-box image was input to the R-CLO model.

The R-CLO model detected and classified the clothing that the participants were wearing. Several results are presented in Fig. 7. Fig. 7(a) shows the example of the accurately classified output for each ensemble of Step C in Fig. 5. Because the images of the participant on the test bed were recorded from two distinct angles, the images for Cams 1 and 2 are shown separately in Fig. 7(a).

Fig. 7(b) shows the types of errors that emerged during the measurement. Error 1 corresponds to situations in which some of the clothes were not detected owing to the participant's pose. Although certain instantaneous postures may lead to a temporal inaccuracy, clothes may be detected correctly in the image obtained from the opposite side. Therefore, this error can be compensated using the image measured from the opposite side. Error 2 corresponded to scenarios in which a garment was erroneously classified as that with a similar insulation area. For instance, in the Tops category, a t-shirt (G3) was classified as a short-sleeve shirt (G1), and a long-sleeve pajama shirt (G14) was classified as a regular long-sleeve shirt (G2). In the Bottoms category, ankle-length skirt (G8) and pajama trousers (G15) were classified as regular trousers (G6).

If the rate of occurrence of the same error was not high, it was treated as an outlier by the control algorithm (Fig. 5) and did not affect the determination of the representative I_{cl}. The results of representative I_{cl} by the control algorithm that were determined every 10 min during experiments of 40 min per ensemble are shown in Fig. 8. Fig. 8 shows the average value of the estimated I_{cl} during the experiment for all participants and the 99% confidence interval of each participant for different ensembles.

The average error for E5 and E7 was 0.1 clo, higher than that of the other ensembles. In several instances, long-sleeve shirt (G2) and suit jacket (G11) were classified as long-sleeve sweater (G4). The average I_{cl} error throughout the experiment was 0.04 clo, and except for E5 and E7, all clothing ensembles corresponded to reduced average I_{cl} errors of 0.02 clo. Overall, the total I_{cl} error was not excessively large. These findings highlighted that the impact of the momentary inaccuracy shown in Fig. 7(b) can be decreased by applying the control algorithm that estimates the representative I_{cl} with the highest classification ratio during the control period.

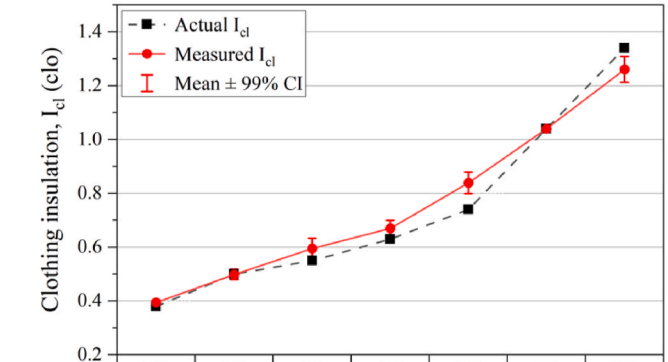

	E1	E2	E3	E4	E5	E6	E7
Actual I_{cl}	0.38	0.5	0.55	0.63	0.74	1.04	1.34
Measured I_{cl}	0.39	0.5	0.59	0.67	0.85	1.04	1.24

Fig. 8. Accuracy of real-time I_{cl} measured in the experiment.

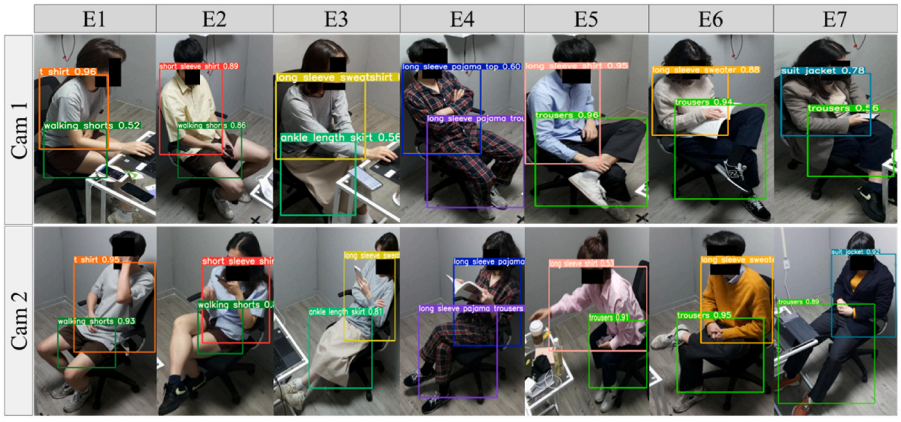

(a) Accurate classification results by ensembles

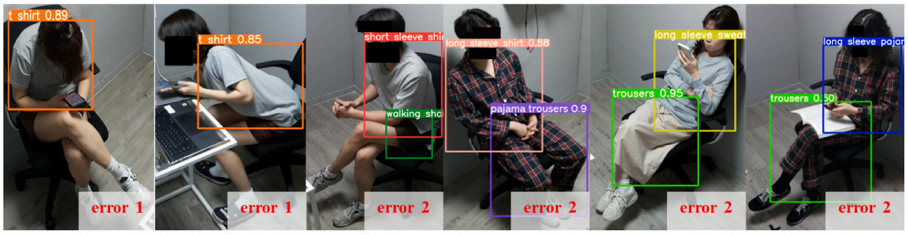

(b) Examples of major errors

Fig. 7. Results of the R-CLO model.

4.2. Experimental results in the heating period

4.2.1. Thermal environment and comfort in the heating period

Data recorded between 10 and 40 min of the experiment were analyzed, with the first 10 min considered the experimenter's adaptation time. Fig. 9 shows the controlled indoor temperature and thermal comfort of the participants based on their clothing ensemble. As shown in Fig. 9(a), the indoor temperatures in Cases 1 and 2 did not change with I_{cl}, with overall average temperatures of 22.5 °C and 24.6 °C, respectively. The average temperature between the two control methods differed by approximately 2 °C. In contrast, as the I_{cl} increased from E1 to E7 in Case 3, the indoor temperature steadily decreased from 26.7 °C to 24.0 °C. In other words, the room temperature was lowered as the clothing became thicker. The indoor temperature in Case 3 was the highest among the three control methods for all other ensemble conditions except E7.

Fig. 9(b) shows the change in the PMV in the controlled environment. The PMV between Cases 1 and 2 differed significantly across ensembles. The PMV difference between E1 and E7 was 2.4 (Case 1) > 1.9 (Case 2) > 0.8 (Case 3). Case 1 was uncomfortable for the occupants in terms of the PMV in all clothing scenarios except E7. The PMV of Case 1 was −2.3, particularly in E1, suggestive of an extremely cold environment with a "cold– very cold" rating. The participants expressed discomfort in Case 2 when the insulation was 0.64 clo or less (E1–E4) because the indoor temperature corresponded to the "slightly cool–cold" state. Although a difference of up to 0.8 PMV was observed in Case 3, the average PMV remained within an acceptable comfort range regardless of the clothing ensemble. This finding highlighted that only Case 3 could provide a comfortable indoor environment in every clothing scenario, especially in low I_{cl} conditions such as E1–E4. In other words, the proposed method corresponded to the most favorable PMV.

The distributions of all TSV data measured throughout the experiment in intervals of 2-min are shown as a box plot in Fig. 9(c) to compare the difference between the TSV and PMV results. The boxed area

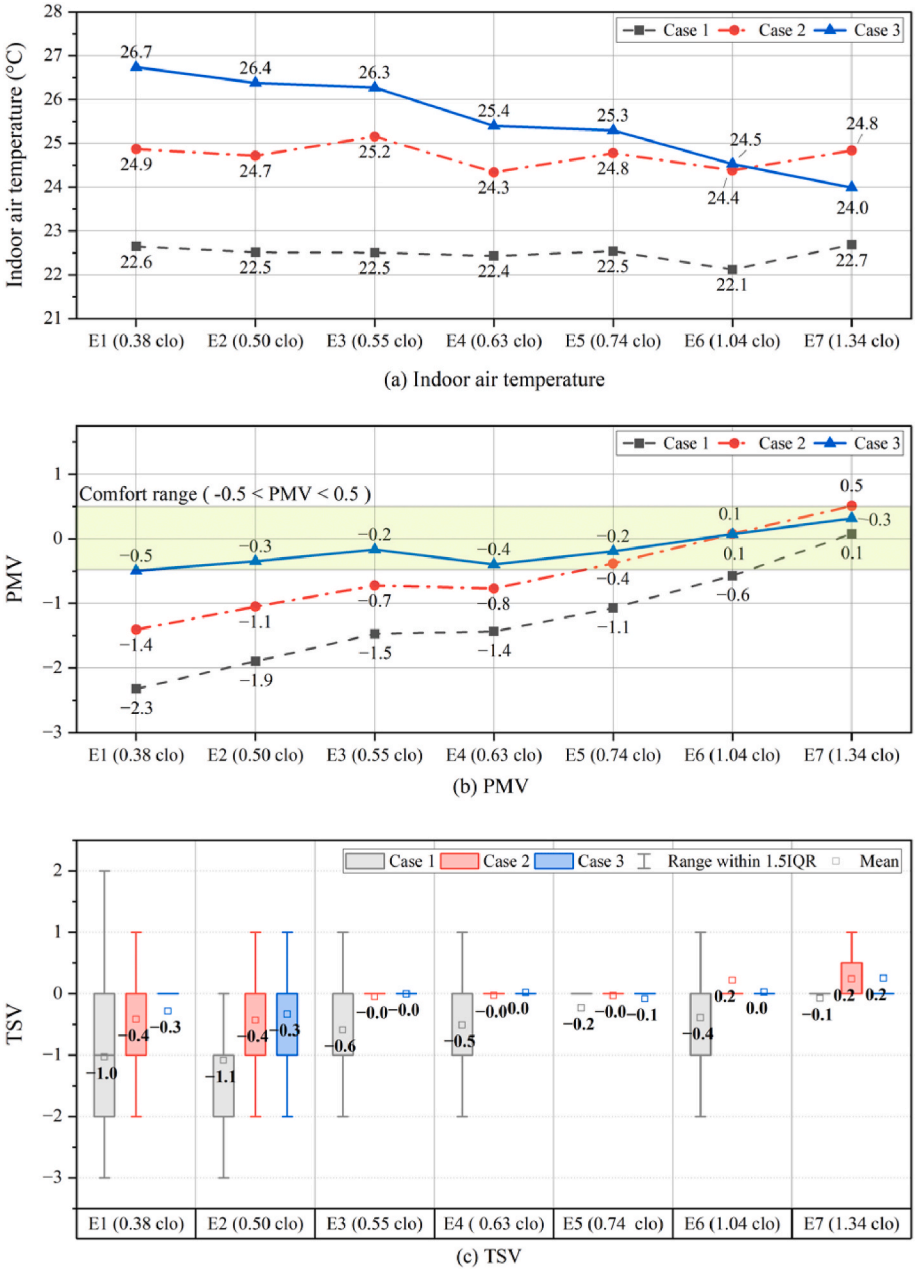

Fig. 9. Results of thermal environment and comfort for different control cases.

represented 25–75% of the total data. Case 1 showed the widest distribution of TSV data in all ensembles except for E5 and E7. The average TSVs of E1 and E2 were −1.0 and −1.1, respectively, indicating that the occupants felt slightly cold. A few participants responded with scores of even −3. Even in Case 2, 50% of the responses in E1 and E2 were between −1 < TSV <0, and the average TSV was −0.4.

The smallest data distribution range was found in Case 3, in which constant TSV data were collected. The data for most of the ensembles belonged to TSV 0, and the average value, including outliers, ranged between −0.3 and 0.2. Specifically, Case 3 provided the occupants with the highest level of actual thermal comfort across all clothing conditions among the three control methods.

The average TSV showed a higher value than the calculated PMV (Fig. 9(b)). In the case of E1, for instance, the PMV was estimated to be −2.4 in Case 1, but the average TSV was −1.0. Additionally, the average TSV was −0.5 or higher for the range of −1.4 to −0.5 PMV. This finding demonstrated that even if the PMV is estimated as a value slightly beyond the comfort range, the comfort of the occupants would be maintained.

Case 3 demonstrated PMV-based control capabilities comparable to the occupant's TSV. Specifically, the occupants were comfortable when the PMV was within the comfort zone. This finding highlighted that the comfort of the actual occupants can be satisfied while reducing the power consumption even if the PMV setpoint of the heating period is set to be lower than zero without deviating from the comfort range. However, this phenomenon occurs only in control methods such as Case 3 in which the actual TSV can be matched to the PMV setting.

4.2.2. Power consumption in the heating period

The power consumption for 30 min during the heating experiment was evaluated to examine the energy requirements for different control methods. The results are shown in Fig. 10. The total power required for each ensemble is shown in Fig. 10(a), and Fig. 10(b) provides examples of certain participants wearing ensembles E1 and E7 to clarify the power consumption per minute.

Regardless of the I_{cl}, the average total power consumption for Cases 1 and 2 was maintained at 125.4 Wh and 144.2 Wh, respectively (Fig. 10 (a)). Approximately 15% more power was used in Case 2 than in Case 1. In contrast, Case 3 exhibited a notable variance in the power consumption based on the clothing insulation. Among the three cases, Case 3 exhibited the largest power consumption in E1 to E5 with low I_{cl}. The power consumption was 75–162% and 44–133% higher than those in Cases 1 and 2, respectively. Case 2 consumed the most power in E6 and E7. For E7 (maximum I_{cl}), the power consumption in Case 3 was 23% and 27% lower than those in Cases 1 and 2, respectively. In other words, the power consumption in Case 3 with insulation values higher than 1.0 clo was lower than that associated with traditional methods.

The power consumption in Case 3 for E4 was higher than for E3 because on many days, the outside temperature in Case 3 was low during the experiment. To examine the variation in the power consumption, the rate of change in power consumption in units of 0.1 clo was determined. Except for E4, the power consumption reduced by approximately 11.6% for an increase of 0.1 clo.

The trend of the power consumption was similar to that of the indoor temperature but not exactly proportional. For E1, the average indoor temperatures in Cases 1, 2, and 3 were 22.6 °C, 24.9 °C, and 26.7 °C,

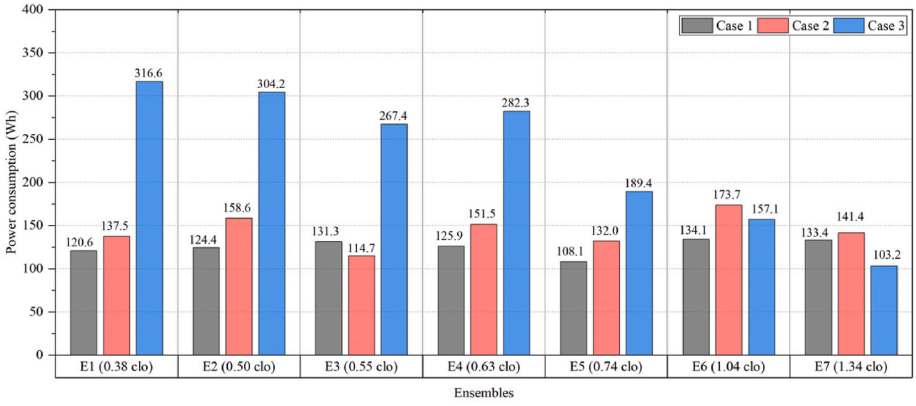

(a) Total power consumption in different control cases

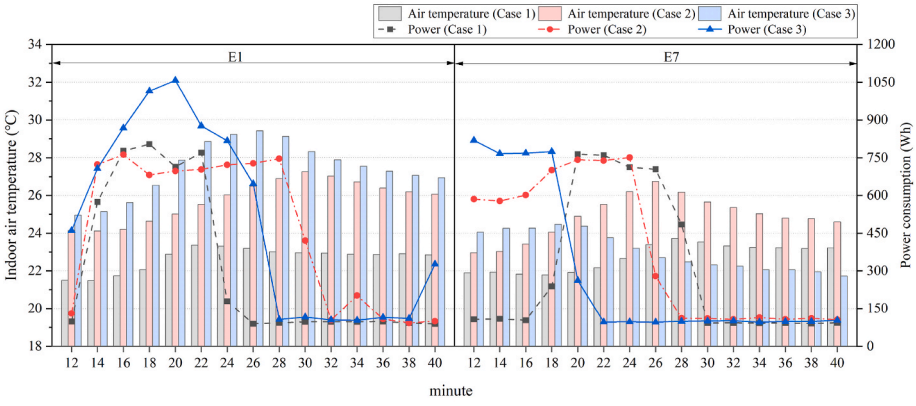

(b) Power consumption distribution across time (on the minute scale)

Fig. 10. Power consumption results.

respectively (Fig. 9(a)). Although, the temperatures in Cases 2 and 3 were 2 °C and 4 °C higher than that in Case 1, the power consumption was 16.9 Wh and 179.1 Wh higher, corresponding to a difference of 10 times. This difference likely occurred because the initial temperature of the test bed was set as 22 °C before the experiment. The power consumption rapidly increased to raise the room temperature in the early stages when the difference between the indoor T_a and T_{set} was large.

This phenomenon can be explained by Fig. 10(b). Fig. 10(b) shows the variation in the room temperature and power consumption at 2-min intervals in the E1 (0.38 clo) and E7 (1.34 clo) experiments of a specific participant. For E1 (0.38 clo), Case 3 set the indoor temperature to 29 °C considering I_{cl}. Thus, the initial power consumption increased rapidly compared with those in the other two control methods. For E7 (1.34 clo), T_{set} was 23–24 °C, and the power consumption decreased first among the control methods. Later, the system's standby power was used.

5. Comparative analysis in seasons

By integrating the results of the cooling period [23], the PMV-based control strategy associated with the R-CLO was analyzed to highlight seasonal variations. The variation in the occupants' thermal comfort and power consumption were also assessed. Five ensembles that were equally worn in both experiments were used to compare the results for the two seasons. The I_{cl} values of the five clothing ensembles were 0.38 clo, 0.50 clo, 0.55 clo, 0.74 clo, and 1.04 clo. Thirty-eight participants were involved in the experiment, with 23 and 15 subjected to heating and cooling, respectively. The average outdoor temperature was 2.2 °C and 24.7 °C in the heating and cooling periods, respectively.

5.1. Thermal environment and comfort

T_{set} was determined differently depending on the control method. In Case 1, T_{set} of the cooling and heating periods were fixed as 25 °C and 22 °C, respectively. In Case 2, T_{set} was set as 26 °C in the cooling period and in the range 23–26 °C in the heating period. In Case 3, the cooling and heating temperatures were varied as 23–27 °C and 21–29 °C, respectively. Because the R-CLO and environmental variables were considered, the range of T_{set} was the widest for Case 3, among the control methods.

The change in the indoor temperature according to the T_{set} for each control case is shown on the left side of Fig. 11. In Case 1, the highest difference in the average indoor temperature for summer and winter was more than 2 °C, whereas the differences for Cases 2 and 3 (PMV-based control methods) were 0.5 °C and 1.0 °C, respectively. In both seasons, Case 3 was the only control method to gradually lower the indoor temperature as I_{cl} increased.

In terms of the PMV (right side of Fig. 11), Cases 1 and 2 showed a significant seasonal difference in PMV and mostly created unpleasant environments with PMV -0.5 or below in winter. Only Case 3 could create an environment that was comfortable in all clothing scenarios in both seasons. Especially in winter, the PMV in Case 3 was improved by up to 1.8 at the lowest I_{cl} (0.38 clo) compared with that of Case 1.

The TSV for both seasons were surveyed in 2-min intervals, and 3313 and 5733 votes were collected in summer and winter, respectively. To facilitate comparison of the TSV data, Fig. 12 shows the TSV distribution for 31 participants (winter: 22, summer: 9) with TSVr values of zero. Note that the figure shows the overall TSV distributions across seasons and ensemble.

A condition of TSV 0, i.e., a thermally neutral state, was considered the comfort state in this analysis. The comfort rate (when TSV = 0) exhibited the following order in both seasons: Case 3 > Case 2 > Case 1. Additionally, the difference in the comfort rate across the control cases was greater in winter than that in summer. In summer, the comfort rate for Case 3 was 81.7%, approximately 14% higher than that of Case 1 (67.4%) and comparable to that of Case 2 (80.8%). In winter, the comfort rate in Case 3 was 76.3%, which was 28.4% and 9.4% higher than in Case 1 (47.9%) and Case 2 (66.9%). In other words, PMV-based control based on the R-CLO provided the optimal comfort environment for occupants in both seasons, and the occupant comfort was significantly enhanced in winter.

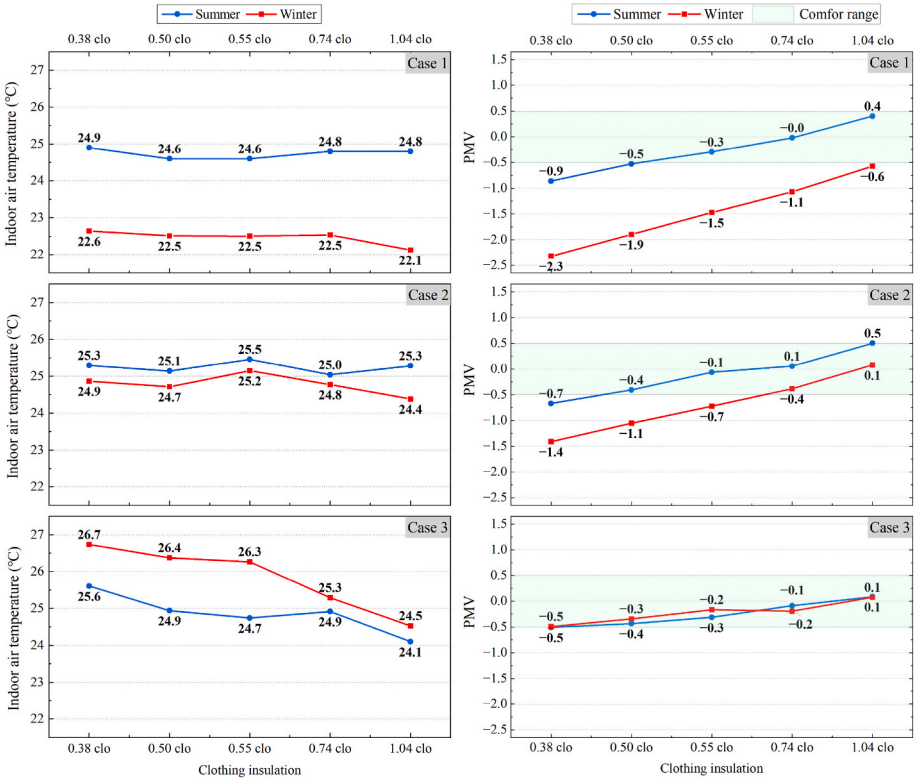

Fig. 11. Comparison of seasonal indoor temperature and PMV.

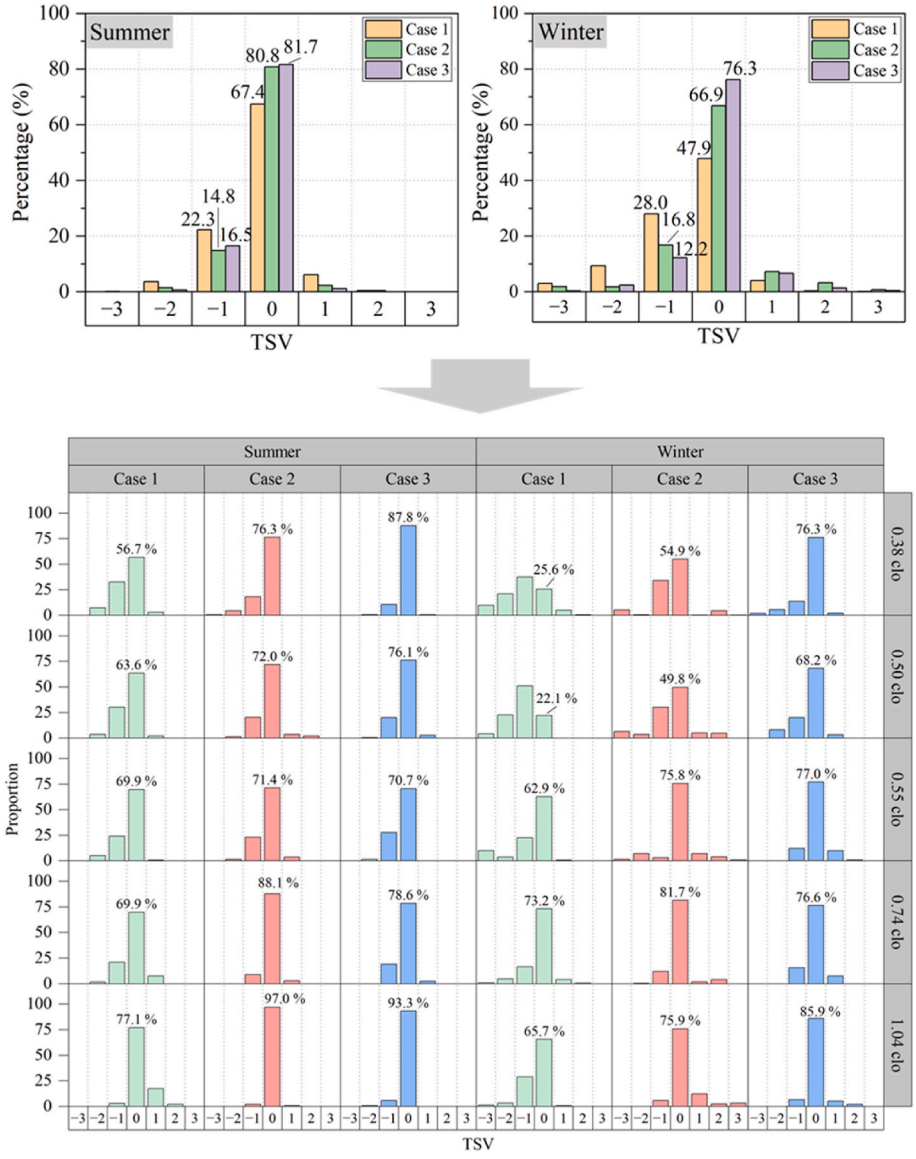

Fig. 12. TSV distributions by seasons and ensembles.

For a more extensive analysis, the lower graph in Fig. 12 shows the distribution of TSV by season according to the clothing ensemble. The TSV distribution of Case 3 was comparable to that of Case 2 in all I_{cl} scenarios, with the highest comfort rate in summer being 87.8% (for 0.38 clo) and 76.1% (for 0.50 clo). However, compared with Case 1, the TSV of Case 3 was significantly enhanced with all I_{cl} conditions, and it improved the comfort rate by up to 31%.

In winter, for all I_{cl} except 0.74 clo, Case 3 achieved the highest comfort rate. In contrast, the comfort in Cases 1 and 2 was significantly decreased when the I_{cl} was low (0.38 clo and 0.50 clo). For the lowest I_{cl} (0.38 clo), the comfort in Case 3 was 50.7% and 21.4% higher than those in Cases 1 and 2, respectively. In other words, in winter, the traditional methods (Cases 1 and 2), which are typically used for controlling buildings, may be disadvantageous in terms of thermal comfort in most clothing conditions compared to Case 3. Therefore, the proposed method can best maintain a comfortable environment in most I_{cl} conditions regardless of the season.

5.2. Power consumption

The power consumption in each season is shown in Fig. 13. The average power consumption for the experiment (30 min per participant) according to I_{cl} is shown as a stacked bar chart for different seasons. The total power consumption is specified in each block, and the data for Cases 1 and 2 also include the change rate in comparison with Case 3.

The ratio of power consumption in Case 3 varied with I_{cl}. When I_{cl} increased, for maintaining the indoor temperature at a low value, the power consumption increased in summer and decreased in winter. In contrast, the other two control methods exhibited a relatively constant distribution of power consumption regardless of changes in I_{cl}.

In summer, the power consumption in Case 3 was 2.9–49.4% lower than that in Case 1, except at the highest I_{cl} (1.04 clo). Compared with Case 2 that had a fixed I_{cl} value of 0.50 clo in summer, the power consumption in Case 3 was 2.8–18.1% lower when the I_{cl} was below 0.5 clo. In winter, Case 3 consumed the highest power for all clothing types except at 1.04 clo, and more than twice the power was consumed compared to those in the other cases at the lowest I_{cl} (0.38 clo).

Overall, depending on the clothing, the power consumption of Case 3 in summer varied from −33.1% to +38% compared with those of the existing control methods. Especially in winter, the difference in the power consumption based on clothing was significant. A comparison of Case 3 to the other cases showed that power consumption might vary

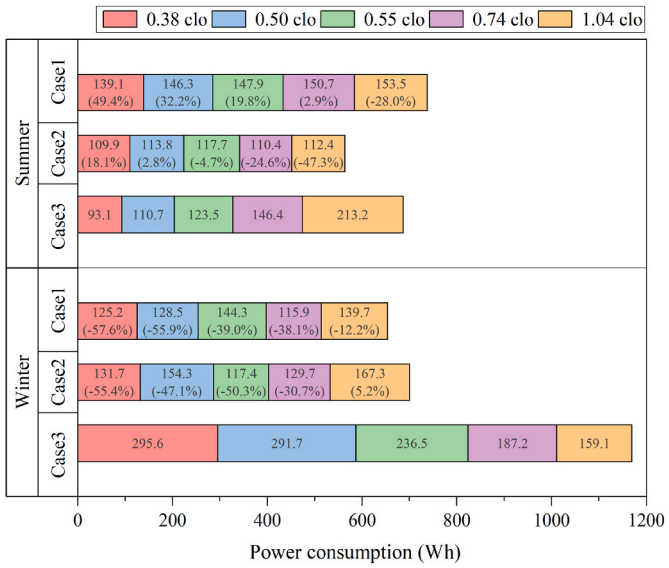

Fig. 13. Total power consumption across seasons.

from −5% to 2.3 times. Depending on the type of clothing donned by the occupants, the energy consumption may be higher or lower than those of the existing control methods. As demonstrated in Fig. 12, Case 3 serves to provide a comfortable environment to the occupants in accordance with I_{cl}. In contrast, the existing control strategies appear to prioritize energy over comfort, particularly during the winter. In other words, traditional control methods may consume less power during system operation; however, they may induce an uncomfortable environment for the occupants.

The ratio of power consumption in Case 3 was converted to 0.1 clo units to quantify the variation in the power consumption. The power consumption in summer and winter could be reduced on average by 16% and 13.7%, respectively, when the insulation changed by every 0.1 clo. To explain in detail, a decrease of 0.1 clo in summer the power saved about 16% and an increase of 0.1 clo in winter the power saved about 13.7%. In conclusion, depending on I_{cl}, the proposed control method may be profitable or disadvantageous in terms of the power consumption. For example, if occupants wear only 0.38 clo in summer, the comfort can be improved, and power consumption can be reduced. If 0.38 clo clothes are worn in winter, a comfortable thermal environment can be obtained, but the power consumption may be two times that of the existing method. In other words, even when the proposed control method can consume more power than the existing control methods in some case, it ensures a comfortable environment for occupants.

Therefore, a reasonable tradeoff between the power consumption and thermal comfort must be ensured based on the clothing information. For example, the operation of auxiliary systems can be considered by adjusting other parameters that determine the PMV in addition to the room temperature through a personal comfort system (PCS) [48] such as cooling/heating radiant panels or floor based ventilation systems [49] with adjustable air velocity.

6. Conclusions

This paper proposes a control algorithm embedding the R-CLO model that can detect occupants and estimate the real-time I_{cl} through RGB images, as a new OCC strategy for improving the occupant comfort. The effect of R-CLO information on the comfort and power consumption was analyzed by conducting a control experiment by applying the proposed algorithm. The following conclusions were derived.

1) The proposed model first recognizes humans and then uses the R-CLO model that can classify more than 34 clothing ensembles based on 16 garments to estimate the real-time clothing insulation. The R-CLO model exhibited a classification accuracy of more than 80% for 7 out 11 garments and outperformed the original model. The proposed control algorithm could estimate the representative I_{cl} value of the control period with an average error of 0.04 clo, thereby accurately reflecting the actual value.
2) According to the results of the winter experiment, the proposed method based on the R-CLO yielded PMV values that satisfied the comfort range in all clothing conditions. The survey results of occupants' TSV indicated that system control induced a comfortable environment, outperforming the existing methods by 9.4–28.4%. Moreover, the power consumption of the proposed method was 9.5–27.0% lower than that of the existing control method for clothes with insulation values of 1.0 clo or higher.
3) According to the seasonal assessment, the proposed control method improved thermal comfort in both winter and summer. The TSV comfort rate increased by 14.3% and 28.4% in the summer and winter, respectively. In addition, the change in clothing insulation resulted in a noticeable variation in the power consumption. The average power consumption from the experiments in summer and winter were reduced on average by 16% and 13.7%, respectively, when the insulation changed by every 0.1 clo.

Overall, the proposed method can maintain thermal comfort for all types of occupant clothing, although the power consumption may vary. To simultaneously ensure thermal comfort and reduce the power consumption, it may be necessary to use an innovative energy-saving strategy such as relaxing the PMV setpoint within the comfort range and using auxiliary systems or PCSs to adjust other PMV parameters. To this end, experiments must be performed for a variety of systems and building sizes, and the effectiveness of the strategies must be analyzed.

To improve the overall garment classification accuracy and expand its applicability, the R-CLO model must be continuously trained over data pertaining to various clothing, indoor environments, camera angles, and resolutions. The current model cannot effectively identify the specifics of the inner garments because it relies solely on image data. Therefore, to increase the model's applicability, the total clothing insulation must be corrected assuming the occupant's clothing layer while considering relevant information such as the temperature difference between the skin and clothing, detected clothing, and seasonal information. Additionally, the objectivity and accuracy of thermal comfort estimation can be enhanced by combining the R-CLO model with a model that identifies the occupants' discomfort through human gestures or poses.

In this context, future studies can focus on the following aspects: The optimal I_{cl} for representing multiple occupants must be determined using the proposed control approach for comfort control in multi-use facilities. Additionally, occupant metabolic rate must be considered along with the clothing insulation to achieve accurate and practical PMV-based comfort control. To this end, an approach for estimating the real-time metabolic rate with an image-based object recognition model can be applied. The human pose estimation model can estimate the posture based on the joint coordinates of the person detected in the image and use it to infer the metabolic rate [19,50]. To accurately measure the thermal comfort, further experiments must be conducted by considering the real-time data of the two personal factors.

CRediT authorship contribution statement

Eun Ji Choi: Writing – review & editing, Writing – original draft, Visualization, Software, Methodology, Formal analysis. **Young Jae Choi:** Visualization, Validation, Software, Investigation. **Nam Hyeon Kim:** Visualization, Validation, Software, Methodology. **Jin Woo Moon:** Supervision, Project administration, Methodology, Funding acquisition,

Formal analysis, Conceptualization.

Declaration of competing interest

The authors declare that they have no known competing financial interests or personal relationships that could have appeared to influence the work reported in this paper.

Data availability

The authors are unable or have chosen not to specify which data has been used.

Acknowledgments

This work was supported by the National Research Foundation of Korea (NRF) grant funded by the Korea government (MSIT) (2019R1A2C1084145) and Korea Institute of Energy Technology Evaluation and Planning (KETEP), Ministry of Trade, Industry & Energy (MOTIE) of the Republic of Korea (No. 20212020800120).

Appendix AParticipants and garments used in the experiment

This appendix presents the information of the participants and clothes worn in the experiment. Table A1 summarizes the details of the twenty-three participants, i.e., the gender, height, weight, age, BMI, number of surveys, period of participation, and TSVr information. The lack of TSVs indicates a technical issue encountered in the experiment (e.g., internet connectivity). Male and female participants voted 347–380 and 412–450 times, respectively. ISO 9920 [36] was used as the basis for setting the garments used in this study. Table A2 presents the selected garment types and fabric conditions. To the greatest extent possible, the clothing used in the experiment was prepared to comply with the settings presented in Table A2 to satisfy the insulation value specified by ISO 9920.

Table A1
Participant information

ID	Sex	Height (m)	Weight (kg)	Age	BMI (kg/m^2)	TSVr	Number of surveys	Participation period
1	Male	177	71	25	22.7	0	358	1/17, 1/20
2	Male	170	60	24	20.8	0	365	1/17, 1/18
3	Male	171	73	24	25.0	0	363	1/18, 1/19
4	Male	183	70	22	20.9	0	364	1/19, 1/20
5	Female	153	42	24	17.9	0	429	1/21, 1/28
6	Female	164	50	26	18.6	0	413	1/21, 1/28
7	Female	160	51	23	19.9	0	421	1/24, 1/27
8	Male	183	75	30	22.4	0	380	1/24, 1/27
9	Female	157	52	27	21.2	0	429	1/25, 1/26
10	Female	167	62	22	22.2	0	412	1/25, 1/26
11	Male	169	55	24	19.3	0	368	1/29, 2/5
12	Female	162	50	24	19.1	0	419	2/5, 2/13
13	Male	171	70	29	23.9	0	365	2/7, 2/20
14	Female	158	46	24	18.4	0	446	2/8, 2/10, 2/24
15	Male	168	65	29	23.0	0	360	2/8, 2/10, 2/11
16	Male	168	56	26	19.8	0	357	2/9, 2/11
17	Female	157	51	22	20.7	0	425	2/12, 2/13
18	Female	168	53	20	18.8	0	450	2/15, 2/17
19	Female	163	57	22	21.5	0	422	2/15, 2/17
20	Male	174	58	21	19.2	0	368	2/16, 2/18
21	Male	178	63	23	19.9	0	347	2/21, 2/23
22	Male	175	72	23	23.5	−1	372	2/23, 2/24
23	Female	157	50	29	20.3	0	421	3/5, 3/19

Table A2
Garments used in the experiment (with reference to ISO 9920 [36])

Category	No	Garment type	Garment insulation (I_{clu})	Fabric in ISO 9920	Fabric used in the experiment
Top	56	short-sleeve shirt	0.24	twill weave | cotton | 0.7 mm	100% cotton
	54	long-sleeve shirt	0.33	twill weave | cotton | 0.7 mm	100% cotton
	31	t-shirt	0.10	cotton | 1.5 mm	100% cotton
	142	long-sleeve sweater	0.36	jersey/weft knit | 85% wool, 15% nylon | 3.55 mm	(male) 78% wool, 22% nylon (female) 45% wool, 30% nylon, 15% polyester, 5% mix
	37	long-sleeve sweatshirt	0.16	cotton, wool	100% cotton
Bottom	109	trousers (straight, loose)	0.22	cotton | 1.0 mm	100% cotton
	304	knee-length skirt	0.14	denim/twill weave | 100% cotton | 0.8 mm	100% cotton
	300	ankle-length skirt	0.23	denim/twill weave | 100% cotton | 0.8 mm	100% cotton
	97	walking shorts	0.08	denim/twill weave | 100% cotton | 0.8 mm	(male) 97% cotton, 3% span (female) 60% cotton, 40% linen

(*continued on next page*)

Table A2 (*continued*)

Category	No	Garment type	Garment insulation (I_{clu})	Fabric in ISO 9920	Fabric used in the experiment
	291	sweatpants	0.28	fleece-backed double knit | 50% polyester, 38% cotton, 12% viscose	(male) 52% cotton, 48% polyester (female) 100% cotton
Outer	156	suit jacket	0.36	denim/twill weave | 100% cotton | 0.8 mm	(male) 56% cotton, 44% polyester (outside)/100% polyester (inside) female) 63% polyester, 34% rayon, 3% span (outside)/60% polyester, 40% cotton (inside)
Dress	333	short-sleeve shirt dress	0.29	broadcloth/plain weave | 65% polyester, 35% cotton | 0.38 mm	35% cotton, 65% polyester
	332	long-sleeve shirt dress	0.35	broadcloth/plain weave | 65% polyester, 35% cotton | 0.38 mm	50% cotton, 50% polyester
Pajama	359	long-sleeve pajama top	0.31	broadcloth/plain weave | 65% polyester, 35% cotton | 0.38 mm	50% cotton, 50% polyester
	362	pajama trousers	0.17	broadcloth/plain weave | 65% polyester, 35% cotton | 0.38 mm	50% cotton, 50% polyester
	361	short-sleeve pajama top	0.25	broadcloth/plain weave | 65% polyester, 35% cotton | 0.38 mm	50% cotton, 50% rayon

References

[1] T. Hong, H.-W. Lin, Occupant Behavior: Impact on Energy Use of Private Offices, Lawrence Berkeley National Lab.(LBNL), Berkeley, CA (United States), 2013.

[2] J. Langevin, P.L. Gurian, J. Wen, Tracking the human-building interaction: A longitudinal field study of occupant behavior in air-conditioned offices, J. Environ. Psychol. 42 (2015) 94–115.

[3] T. Yang, A. Bandyopadhyay, Z. O'Neill, J. Wen, B. Dong, From occupants to occupants: a review of the occupant information understanding for building HVAC occupant-centric control, Build Simul-China 15 (6) (2022) 913–932.

[4] S. Naylor, M. Gillott, T. Lau, A review of occupant-centric building control strategies to reduce building energy use, Renew. Sustain. Energy Rev. 96 (2018) 1–10.

[5] S. Carlucci, M. De Simone, S.K. Firth, M.B. Kjaergaard, R. Markovic, M.S. Rahaman, M.K. Annaqeeb, S. Biandrate, A. Das, J.W. Dziedzic, G. Fajilla, M. Favero, M. Ferrando, J. Hahn, M. Han, Y. Peng, F. Salim, A. Schluter, C. van Treeck, Modeling occupant behavior in buildings, Build. Environ. 174 (2020).

[6] W. O'Brien, A. Wagner, M. Schweiker, A. Mahdavi, J. Day, M.B. Kjaergaard, S. Carlucci, B. Dong, F. Tahmasebi, D. Yan, T.Z. Hong, H.B. Gunay, Z. Nagy, C. Miller, C. Berger, Introducing IEA EBC annex 79: key challenges and opportunities in the field of occupant -centric building design and operation, Build. Environ. 178 (2020).

[7] F. Jazizadeh, A. Ghahramani, B. Becerik-Gerber, T. Kichkaylo, M. Orosz, Human-building interaction framework for personalized thermal comfort-driven systems in office buildings, J. Comput. Civ. Eng. 28 (1) (2014) 2–16.

[8] J.Q. Xie, H.Y. Li, C.T. Li, J.S. Zhang, M.H. Luo, Review on occupant-centric thermal comfort sensing, predicting, and controlling, Energy Build. (2020) 226.

[9] Y.J. Choi, B.R. Park, J.Y. Hyun, J.W. Moon, Development of occupancy prediction model and performance comparison according to the recurrent neural network models, J. Architect. Instit. Korea 38 (10) (2022) 10.

[10] B. Gunay, Z. Nagy, C. Miller, M. Ouf, B. Dong, Using occupant-centric control for commercial HVAC systems, ASHRAE J. 63 (2021) 30–40.

[11] ISO 7730:2005, Ergonomics of the Thermal Environment — Analytical Determination and Interpretation of Thermal Comfort Using Calculation of the PMV and PPD Indices and Local Thermal Comfort Criteria, European Committee for Standardization, UK, 2005.

[12] ASHRAE standard 55, thermal environmental conditions for human occupancy, in: American Society of Heating, Refrigerating and Air-Conditioning Engineers, Atlanta, GA, USA, 2020.

[13] Cen, Indoor Environmental Input Parameters for Design and Assessment of Energy Performance of Buildings: Addressing Indoor Air Quality, Thermal Environment, Lighting and Acoustics. EN 15251, European Committee for Standardization, Brussels, 2007.

[14] P.O. Fanger, Thermal Comfort. Analysis and Applications in Environmental Engineering, Danish Technical Press, Copenhagen, 1970.

[15] C. Zhong, J.H. Choi, Development of a data-driven approach for human-based environmental control, in: 10th International Symposium on Heating, Ventilation and Air Conditioning (ISHVAC), PEOPLES R CHINA, Jinan, 2017, pp. 1665–1671.

[16] J.H. Choi, V. Loftness, Investigation of human body skin temperatures as a bio-signal to indicate overall thermal sensations, Build. Environ. 58 (2012) 258–269.

[17] W.T. Sung, S.J. Hsiao, The Application of Thermal Comfort Control Based on Smart House System of IoT, Measurement, 2020, p. 149.

[18] C. Qin, W.R. Zhou, H.Q. Fang, W.Z. Lu, E.W. Lee, Optimization of return vent height for stratified air distribution system with impinging jet supply satisfying threshold of vertical bar PMV vertical bar < 0.5, J. Clean. Prod. 359 (2022).

[19] E.J. Choi, J.W. Moon, J.H. Han, Y. Yoo, Development of a deep neural network model for estimating joint location of occupant indoor activities for providing thermal comfort, Energies 14 (3) (2021).

[20] I. Mutis, A. Ambekar, V. Joshi, Real-time Space Occupancy Sensing and Human Motion Analysis Using Deep Learning for Indoor Air Quality Control, 116, Automat Constr, 2020.

[21] J.S. Liu, I.W. Foged, T.B. Moeslund, Clothing insulation rate and metabolic rate estimation for individual thermal comfort assessment in real life, Sens. Basel 22 (2) (2022).

[22] H. Choi, B. Jeong, J. Lee, H. Na, K. Kang, T. Kim, Deep-vision-based metabolic rate and clothing insulation estimation for occupant-centric control, Build. Environ. 221 (2022).

[23] E.J. Choi, B.R. Park, N.H. Kim, J.W. Moon, Effects of thermal comfort-driven control based on real-time clothing insulation estimated using an image-processing model, Build. Environ. 223 (2022), 109438.

[24] R.T. Ogulata, The effect of thermal insulation of clothing on human thermal comfort, Fibres Text. East. Eur. 15 (2) (2007) 67–72.

[25] Y. Tang, Z.X. Su, H. Yu, K.G. Zhang, C.E. Li, H. Ye, A Database of Clothing Overall and Local Insulation and Prediction Models for Estimating Ensembles' Insulation, 207, Build Environ, 2022.

[26] ISO 15831:2004,, Clothing — Physiological Effects — Measurement of Thermal Insulation by Means of a Thermal Manikin, ISO, Switzerland, 2004.

[27] P.M. de Carvalho, M.G. da Silva, J.E. Ramos, Influence of weather and indoor climate on clothing of occupants in naturally ventilated school buildings, Build. Environ. 59 (2013) 38–46.

[28] K.H. Lee, S. Schiavon, Influence of three dynamic predictive clothing insulation models on building energy use, HVAC sizing and thermal comfort, Energies 7 (4) (2014) 1917–1934.

[29] F. Haldi, D. Robinson, Modelling occupants' personal characteristics for thermal comfort prediction, Int. J. Biometeorol. 55 (5) (2011) 681–694.

[30] S. Schiavon, K.H. Lee, Dynamic predictive clothing insulation models based on outdoor air and indoor operative temperatures, Build. Environ. 59 (2013) 250–260.

[31] J.H. Lee, Y.K. Kim, K.S. Kim, S. Kim, Estimating clothing thermal insulation using an infrared camera, Sens. Basel 16 (3) (2016).

[32] J. Miura, M. Demura, K. Nishi, S. Oishi, Thermal comfort measurement using thermal-depth images for robotic monitoring, Pattern Recogn. Lett. 137 (2020) 108–113.

[33] S. Lu, E. Cochran Hameen, Integrated IR Vision Sensor for Online Clothing Insulation Measurement, 2018.

[34] J.S. Liu, I.W. Foged, T.B. Moeslund, Automatic Estimation of Clothing Insulation Rate and Metabolic Rate for Dynamic Thermal Comfort Assessment, Pattern Anal Appl, 2021.

[35] H. Choi, H. Na, T. Kim, T. Kim, Vision-based estimation of clothing insulation for building control: a case study of residential buildings, Build. Environ. 202 (2021).

[36] B.R. Park, E.J. Choi, Y.J. Choi, J.W. Moon, Development an image recognition-based clothing estimation model for comfortable building thermal controls, J. Architect. Instit. Korea 38 (1) (2022) 8.

[37] ISO 9920, Ergonomics of the Thermal Environment — Estimation of Thermal Insulation and Water Vapour Resistance of a Clothing Ensemble, 2007, 2007. Switzerland.

[38] J.F. Nicol, M.A. Humphreys, Adaptive thermal comfort and sustainable thermal standards for buildings, Energy Build. 34 (6) (2002) 563–572.

[39] M. De Carli, B.W. Olesen, A. Zarrella, R. Zecchin, People's clothing behaviour according to external weather and indoor environment, Build. Environ. 42 (12) (2007) 3965–3973.

[40] H. Matsumoto, Y. Iwai, H. Ishiguro, in: Citeseer MVA (Ed.), Estimation of Thermal Comfort by Measuring Clo Value without Contact, 2011, pp. 491–494.

[41] J. Dziedzic, D. Yan, V. Novakovic, Measurement of Dynamic Clothing Factor (D-CLO), NTNU, Trondheim, 2018.

[42] K. Watanabe, H.B. Rijal, T. Nakaya, Investigation of Clothing Insulation and Thermal Comfort in Japanese Houses, PLEA, 2013.

[43] P.M. Ferreira, A.E. Ruano, S. Silva, E.Z.E. Conceicao, Neural networks based predictive control for thermal comfort and energy savings in public buildings, Energy Build. 55 (2012) 238–251.
[44] G. Jocher, K. Nishimura, T. Mineeva, R. Vilarino, YOLOv5, 2020. https://ultralytics.com/yolov5, 05.
[45] E.A. McCullough, B.W. Jones, J.J.A.T. Huck, A compr. data base estimat clothing insulat. 91 (2) (1985) 29–47.
[46] H.B. Zhang, Y. Chen, J.W. Rui, H. Yoshino, J.F. Zhang, X. Chen, J. Liu, Effects of thermal environment on elderly in urban and rural houses during heating season in a severe cold region of China, Energy Build. 198 (2019) 61–74.
[47] W. Lotens, G.J.E. Havenith, Effects of Moisture Absorption in Clothing on the Human Heat Balance, 38, 1995, pp. 1092–1113, 6.
[48] R. Rawal, M. Schweiker, O.B. Kazanci, V. Vardhan, Q. Jin, D.M. Lin, Personal comfort systems: a review on comfort, energy, and economics, Energy Build. 214 (2020).
[49] F. Bauman, L. Johnston, H. Zhang, E.A. Arens, Performance Testing of a Floor-Based, Occupant-Controlled Office Ventilation System, 1991.
[50] E.J. Choi, Y. Yoo, B.R. Park, Y.J. Choi, J.W. Moon, Development of occupant pose classification model using deep neural network for personalized thermal conditioning, Energies 13 (1) (2020).